Wave aberration of human eyes and new descriptors of image optical quality and visual performance

Marco Lombardo, MD, PhD, Giuseppe Lombardo, Eng PhD

The expansion of wavefront-sensing techniques redefined the meaning of *refractive error* in clinical ophthalmology. Clinical aberrometers provide detailed measurements of the eye's wavefront aberration. The distribution and contribution of each higher-order aberration to the overall wavefront aberration in the individual eye can now be accurately determined and predicted. Using corneal or ocular wavefront sensors, studies have measured the interindividual and age-related changes in the wavefront aberration in the normal population with the goal of optimizing refractive surgery outcomes for the individual. New objective optical-quality metrics would lead to better use and interpretation of newly available information on aberrations in the eye. However, the first metrics introduced, based on sets of Zernike polynomials, is not completely suitable to depict visual quality because they do not directly relate to the quality of the retinal image. Thus, several approaches to describe the real, complex optical performance of human eyes have been implemented. These include objective metrics that quantify the quality of the optical wavefront in the plane of the pupil (ie, pupil-plane metrics) and others that quantify the quality of the retinal image (ie, image-plane metrics). These metrics are derived by wavefront aberration information from the individual eye. This paper reviews the more recent knowledge of the wavefront aberration in human eyes and discusses the image-quality and optical-quality metrics and predictors that are now routinely calculated by wavefront-sensor software to describe the optical and image quality in the individual eye.

Financial Disclosure: Neither author has a financial or proprietary interest in any material or method mentioned.

J Cataract Refract Surg 2010; 36:313–331 © 2010 ASCRS and ESCRS

The eye is an optical system that has several optical elements that focus light rays representing images onto the retina. Imperfections in the components and materials in the eye may cause light rays to deviate from the desired path. These deviations, referred to as optical aberrations, result in blurred images and decreased visual performance.[1] Beyond optical aberrations, dispersion of light, diffraction, and light scattering occur in the human eye.

Submitted: March 11, 2009.
Final revision submitted: September 4, 2009.
Accepted: September 29, 2009.

From IRCCS Fondazione G.B. Bietti (M. Lombardo), Rome, Vision Engineering (G. Lombardo), Rome, and CNR-INFM LiCryL Laboratory (G. Lombardo), Department of Physics, University of Calabria, Rende, Italy.

Corresponding author: Marco Lombardo, MD, PhD, Via Adda 7, Rome, Italy. E-mail: mlombardo@visioeng.it.

During the past decade, rapid improvement in wavefront-related technologies, including the development of sensors for measuring the optical properties of the eye in the clinical environment, has allowed the ophthalmic community to move the wavefront theory of light transmission from an academic concept to one that is central to better understanding of the effect of aberrations on visual performance and the corresponding image-forming properties of the eye.[2,3] Furthermore, efforts in this area of clinical research are leading to the development of innovative systems and devices to improve retinal imaging, such as by adaptive optics,[4] as well as to improve individual visual quality by wavefront-guided laser refractive surgery or personalized contact lenses or intraocular lenses (IOLs).

The imperfections in the optics of the eye are now measured and expressed as wave aberration errors. The wave aberration defines how the phase of light is affected as it passes through the eye's optical system

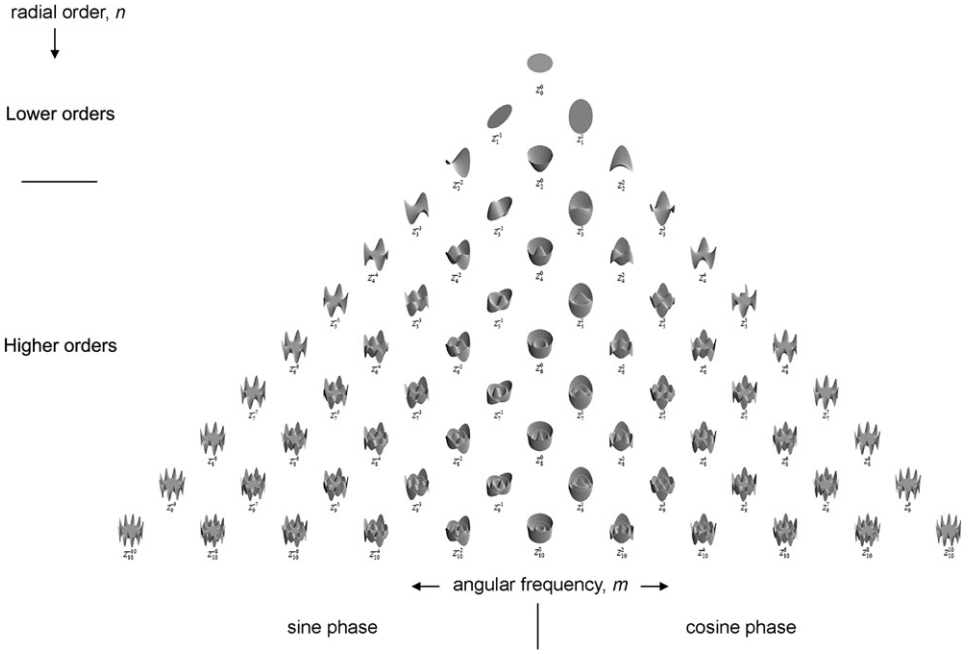

Figure 1. The Zernike pyramid showing polynomials up to the 10th orders. In the double-indexing scheme, Z_n^m, the subscript index n describes the order of the radial polynomial and the superscript index m describes the azimuthal frequency of the sinusoidal component. The 0- to 2nd-order terms represent low optical aberrations in the eye, with 2nd-order terms (ie, defocus and astigmatism) having the highest contribution to the overall wavefront aberration in the eye. Terms of the 3rd order and higher represent the HOAs. The 3rd- and 4th-order terms are the most prevalent HOA in the human eye.

and is usually defined mathematically by a series of polynomials; that is, by Zernike polynomials.[5,6] Zernike polynomials are used to classify and represent optical aberrations because they are made up of terms of the same form as the types of aberrations observed when describing the optical properties of the eye and can be used reciprocally with no misunderstanding. Moreover, the advantage of describing ocular aberrations using the normalized Zernike expansion, generally depicted as a pyramid (Figure 1), is that the value of each mode represents the root mean square (RMS) wavefront error attributable to that mode. Coefficients with a higher value identify the modes (aberrations) that have the greatest impact on the total RMS wavefront error in the eye and thus in reducing the optical performance of the eye.[7] This is not to say, however, that using Zernike polynomials is the best approach for fitting the eye's wavefront aberration data[8] and thus to describe the image and optical quality of the eye. The 2 main practical drawbacks of Zernike polynomials are that they do not show the relative impact of each aberration on visual function and, when considering irregular ocular optics (eg, eyes with keratoconus), they cannot accurately represent the optical properties, resulting in inadequate description of the eye's image-forming properties. Thus, several metrics for quantifying the optical quality of the eye and predicting image optical quality at the fovea have been proposed and grouped in the category of image-plane metrics (eg, point-spread function [PSF], modulation transfer function [MTF]).[9,10]

The scope of this review is to discuss the current knowledge on the optical and imaging properties of the human eye and ways to describe and measure them. The ocular wavefront aberration architecture of the eye, in particular higher-order errors, is described in the first part of the paper; innovative metrics and predictors of visual performance are discussed after a brief introduction of the physical and mathematical description of the main optical concepts needed to understand the significance of metrics. Most objective image- and optical-quality metrics in this review are currently calculated and shown by commercial wavefront sensors and represent a valid tool for evaluating the optical and image quality in the individual eye in the clinical environment.

CAUSES AND SOURCES OF VISION BLURRING IN THE HUMAN EYE

The human eye can be described as a compound lens system consisting of 3 main components: the cornea, the pupil, and the crystalline lens. The cornea (or better, the first corneal surface; that is, the cornea including the tear film) is the first optics of the eye and the dominating structure in the optical power of the eye (mean approximately 70%). Accordingly, it is the main contributor to aberrations in the eye. The anterior cornea has a prolate profile; that is, the central region is steeper than the periphery. This shape helps reduce the amount of spherical aberration in the whole eye. However, corneal shapes vary significantly between individuals and give rise to astigmatism and higher-order asymmetrical aberrations (eg, coma).

The second component, the pupil, regulates the aperture of the eye's image system, influencing the

amount of light that reaches the retina. As in any optical system, the size of the pupil has important consequences for image formation. A smaller pupil increases the depth of focus and minimizes the effects of higher-order aberrations (HOAs) by reducing the size of the blur circle onto the retina, although down to approximately 2.3 mm diameter, then diffraction begins to increase the blur circle and the effect of diffraction.[11] To the contrary, the magnitude of aberrations increases with pupil dilation,[12,13] leading to a decrease in visual performance and optical quality of the retinal image.

Regarding the third component, controlled changes in the shape and thickness of the crystalline lens and in distances between the posterior corneal and anterior lens surfaces allow the eye to accommodate, the process by which the eye focuses on near objects. Overall, these changes contribute an extra 10.0 to 15.0 diopters (D) of refraction in the young adult eye and diminish with aging.

The optical elements described here work in concert to create an image on the retina. The ideal eye would focus the image of the external world precisely at the foveola, regardless of the field angle. In real eyes, however, perfect imaging never occurs. A variable amount of optical aberrations degrades the optical performance of the individual eye. Lower-order aberrations (LOAs) are the predominant optical aberrations in human-eye optics. They account for approximately 90% of the overall wave aberration in the eye. Defocus—positive (hyperopia) or negative (myopia)—is the dominant aberration, followed by astigmatism (orthogonal or oblique). The correction of LOAs with spectacles, contact lenses, or corneal laser surgery significantly improves unaided vision in most cases. On the other hand, it is well established that the human eye has HOAs that cannot yet be accurately corrected with current mainstream optical or surgical treatments. Although HOAs make a small contribution (on average $\leq$10%) to the total variance of the eye's wave aberration, studies[14,15] show the deleterious effect of HOAs on image quality[4,10] and how correction of HOAs can improve visual performance.

The eye also has chromatic aberrations, errors that are the result of dispersion in optical elements of the eye. The index of refraction of the various components of the eye depends on the wavelength of light; thus, white light entering the eye is spread into a spectrum of color. Therefore, chromatic aberration is simply spherical refractive error that depends on wavelength. Chromatic aberrations (dispersion) are traditionally divided into longitudinal and transverse. The former is the variation in axial power with wavelength and is relatively constant between people. The latter is a shift of the image across the image plane with wavelength and varies considerably between people. It is as longitudinal chromatic aberration is the change in focus and transverse chromatic aberration is the change in tip/tilt or prism. Chromatic aberrations undoubtedly limit retinal image quality because the real world is usually polychromatic.

Diffraction is any deviation of light rays from straight lines that cannot be interpreted as reflection or refraction. Diffraction is a fundamental property of the wave nature of light when it passes through an aperture. In the eye, diffraction is an interaction between light passing through the optics of the eye and the edge of the iris. Even in the absence of aberrations, an infinitesimal point cannot be formed on the retina, and this is because of diffraction. In general, because all optical systems, including the eye, have a limiting aperture, it is impossible to build a diffraction-free optical device. It is theoretically possible to improve image quality in an optical system by minimizing aberrations; however, it is impossible to exceed the limits of image quality set by diffraction. Ultimate optical quality is therefore referred to as diffraction limited; that is, limited by diffraction only. Thus, even "perfect" optical systems have an irreducible amount of blurring due to diffraction. Without aberrations, the perfect eye would convert incoming wavefronts into converging spherical waves. Thus, diffraction causes the image of a point to have a finite size; the point image in an eye that is limited only by diffraction is called the Airy disk.

Scattered light also reduces the performance of any optical system, including the eye, in terms of imaging. Scattered light that reaches the retina is called forward scatter, whereas backscatter is scattered light that leaves the eye before hitting the retina. Forward scatter results in a veiling illuminance superimposed on the retinal image; this reduces the contrast in the retinal image and is accepted as a reason for halos and glare disability. Although backscatter does not degrade image formation, it decreases the transmission of light to the retina.[16–19] Sources of scatter are the ocular media and the retina. Scatter in the ocular media is mainly due to diffusion and the loss of transparency in the cornea (including the tear film), the lens (the largest contributor to light scatter), and the humors.[20,21] Scatter within the retina may depend on the fraction of light passing along the photoreceptors and the layer of the retina where the light is reflected[18] (depending on the wavelength of light used).

HIGHER-ORDER WAVEFRONT ABERRATION ARCHITECTURE OF THE HUMAN EYE

The development of wavefront-sensing techniques for vision science has allowed accurate and objective

measurements of the eye's wave aberration in the clinical setting. This has led to numerous studies of normal and diseased eyes that have allowed us to accurately describe the optical quality and image-forming properties of the eye under various conditions. Similarly, the relative contributions of various eye optics (ie, cornea or lens) to the whole wave aberration and the relative interindividual differences or age-related changes have also been evaluated using corneal or ocular wavefront sensors.

Excluding LOAs from this discussion, it is now well known that the form of the ocular wave aberration varies significantly between individuals, presumably depending on surface asymmetries and surface tilts between the optical components of the particular eye and their relative locations with respect to the pupil.[12–14] To date, there is no clear evidence that aberrations are different between emmetropic eyes or ametropic eyes[22,23] or that they vary systematically with the degree of ametropia.[24] The only distinction between eyes is that those with astigmatism tend to have a slightly larger total amount of HOAs than myopic or hyperopic eyes.

Several studies[2,14,25–27] have measured the distribution and contribution of each HOA to the overall wave aberration in the eye. Higher-order aberrations are relatively low and dominated by 3rd-order coma-like aberrations (vertical coma, horizontal coma, oblique trefoil, horizontal trefoil) and spherical aberration. In general, values of individual HOAs in the normal eye are randomly scattered around zero with 2 clear exceptions. The first exception is spherical aberration, which is systematically biased toward positive values. The second exception is oblique trefoil, which usually has a negative value. The range of absolute values of higher Zernike mode numbers decreases systematically. This means that the magnitude of aberration coefficients in any given individual tends to be smaller for higher-order modes than for lower-order modes. However, the higher orders can still have a significant negative influence on image quality when the pupil is large. It is well known that the contribution of HOAs to overall wave aberration increases with pupil size; more precisely, a mean increase of 3% to 14% has been reported for an increase in pupil size from 3.0 mm to 7.0 mm.[13] In general, however, the increase in overall wave aberration with pupil size has been reported to increase to approximately the second power of the pupil radius.[22] This result is not surprising taking into account that most wave aberration is due to the 2nd order (with a square radius dependency). On the other hand, in eyes with optimized visual acuity, a larger visual benefit can be obtained by correcting the HOA over medium and large pupils.[28] This is particularly true for spherical aberration; indeed, the relative contribution of spherical aberration to the overall wave aberration of the eye increases when the pupil dilates, becoming the dominant HOA in degrading optical quality, followed by coma and trefoil.[12,29] In this context, when describing ocular wave aberration, it is highly recommended to specify the pupil size(s) used to calculate the Zernike representation of the wavefront map. On the other hand, given a set of Zernike coefficients over a single pupil size, it is possible to mathematically compute their values for another pupil size, no matter how much smaller than the original pupil.[30,31]

Experimental studies show that each HOA has a different impact on vision and can interact with other aberrations to positively or negatively influence visual performance.[32] For example, modes near the center of the Zernike pyramid (eg, spherical aberration, coma, secondary astigmatism) have a greater effect on visual performance than modes near the edge of the pyramid (modes having high angular frequency). It has also been reported that modes that are 2 radial orders apart and have the same sign and angular frequency (eg, defocus, spherical aberration) tend to combine to increase visual acuity—in other words, to minimize their individual effect on visual performance—whereas modes with the same radial order (eg, spherical aberration, quadrafoil) tend to combine to decrease vision quality.[33]

As mentioned, the whole optical performance of the normal eye is governed by combination of aberrations in the corneal and intraocular optics. Studies[34–36] have found that the total amount of the wave aberration in the whole eye is always less than that in the anterior cornea or the internal optics. The data are explained by compensatory processing between the cornea and the lens.[37] There is strong evidence of compensation for aberrations between the cornea and intraocular optics in cases of astigmatism (horizontal/vertical), horizontal coma, and spherical aberration.[38] The overall result of the compensation process is a reduction in the magnitude of these aberrations at the retinal plane, with possible improvement in image optical quality at the foveola. In most young eyes, the magnitude of aberrations in the cornea and the lens is larger than in the complete eye, indicating that the lens has a significant role in compensating for corneal aberrations, leading to improved retinal images. However, in older persons, the opposite occurs; the lens adds aberrations to the cornea, yielding a complete system with poorer optical quality. Changes in the shape of the anterior cornea and in the shape and size of the lens throughout life may explain the progressive lack of compensation between optics in older eyes.[39–41] Overall, this phenomenon has been related to a decrease in visual performance with aging.

The balance of corneal and internal aberrations is a typical example of coupling of 2 optical systems. In optical engineering, a series of lenses in cascade are usually used to optimize the overall quality of the system. How this optical-quality optimization occurs in the human eye is not yet completely clear. One can imagine an active process or that the compensation is simply a passive consequence of random positioning of the ocular elements. We consider active adaptation to be that occurring during the individual lifespan and passive adaptation as that determined genetically through evolution. In an active mechanism, for instance, the precise modification of lenticular aberration to cancel aberration in the cornea would require a complicated process, even more sophisticated than the one possibly involved in compensating for defocus in the emmetropization process during development.[42] A passive mechanism would simply be determined by the average aberrations present in the cornea and the lens due to the evolutionary process. The distributions of astigmatism and spherical aberration have systematic patterns in the population of eyes; that is, the opposite sign of the spherical aberrations of corneal and internal optics.[38] This may suggest that an evolutionary process occurs to reach an optimum balance for those aberration terms. However, other aberrations, such as coma, seem to be randomly distributed from person to person, favoring a passive-compensation process or perhaps one in which active compensation occurs during development. In an experimental study, Artal et al.[43] showed that if defocus and astigmatism are excluded, eyes with very different geometric features have similar optical performance. This is a remarkable example of an auto-compensating mechanism for the optics in the individual eye. These results may, in part, indicate a passive, geometry-driven mechanism for aberration compensation in the normal young eye, leading to a simple, but extremely robust layout of the optical components in the eye. On the other hand, these results do not completely exclude an active process (or visually guided) of compensation. A combination of both processes could occur. The characterization of the wavefront aberration in human infant eyes and pediatric eyes could provide valuable information on this issue, possibly indicating whether a postnatal refinement process of HOA (emmetropization like) is active in the whole eye. A study by Brunette et al.[44] found that total higher-order RMS wavefront error tends to decrease progressively between the ages of 5 years and 40 years and then increases with age. On the other hand, in a study of eyes of 1-month-old infants,[45] the mean absolute values of lower- and higher-order Zernike coefficients appeared to be very similar between infant eyes and adult eyes, although it is difficult to derive a significant conclusion because of the study's small population and the inability of infants to fixate when aberration measurements are taken.

Particular attention has been paid to the interocular balance of optical aberrations. It is well documented that the corneal topography of right eyes and left eyes has a mirror-image symmetry[46–49] with respect to the vertical plane of the body. Many studies[13,14,24,50–52] report mirror symmetry of higher-order wavefront aberration maps of the anterior cornea as well as the whole-eye optics between eyes, especially for 3rd- and 4th-order terms. Therefore, even though there appears to be a random variation in eye aberration from person to person, many aberrations in the right eye are significantly correlated with their counterparts in the left eye of the same person. Studies suggest a possible relationship between the interocular symmetry of wavefront aberration and cone orientation, which have also been shown to be mirror symmetric between eyes.[53] In addition, Jiménez Cuesta et al.[54] showed how a higher interocular difference in corneal asphericity can lead to a decrease in the contrast sensitivity function measurements, thus negatively influencing binocular visual performance.

An important aspect of ocular aberrations is that the wavefront aberration in the eye is not static but fluctuates over time.[55] The eye's focus fluctuates around its mean level steady-state accommodation with amplitudes of approximately 0.03 to 0.50 D. In addition, there is a general tendency for spherical aberration to change in a negative direction with increases in accommodation (-0.04 μm/D for accommodative levels of 1.0 to 6.0 D), while the other HOAs are not significantly influenced by accommodation.[56,57] The largest source of temporal short-term (seconds and minutes) instability of an HOA is then represented by microfluctuations in accommodation by the lens.[58] During accommodation, there is an increase in anterior curvature centrally and flattening peripherally in the lens. At the same time, the lens thickness increases and the equatorial diameter decreases, factors that may contribute to the change in aberrations. Another cause of fluctuation is local changes in tear-film thickness over the cornea[59] caused by evaporation, blinking, or both. Over a long period of time (the course of the day and between successive days), the wavefront aberration in the eye is sufficiently stable, with no significant changes in the magnitude and contributions of HOAs.

The effect of aging on HOAs in the human eye has also been evaluated in many studies.[41,60–63] The amount of corneal, lenticular, and ocular HOA increases approximately linearly with age.[40,64,65] In the normal cornea of young persons, 3rd-order Zernike terms are the most prevalent HOAs, followed by

spherical aberration.[3] Corneal coma increases significantly with age,[12,24] although there is disagreement between reported corneal spherical aberration results. In general, there is a slight increase in mean spherical aberration with aging. The moderate increase in spherical aberration is related to a change in the asphericity of the cornea over time.[41] The anterior cornea tends to become less prolate with age, whereas no significant or accurate information is available on age-related changes in the posterior corneal shape. The crystalline lens continues to grow throughout life; the central thickness increases and surface curvatures become more curved with age, inducing changes in the asphericity of the anterior and posterior surfaces with a net increase in spherical aberration.[50,52,62] As discussed, the overall result of decoupling of aberrations between the cornea and the internal eye optics and the concurrent increase in the magnitude of the whole-eye wavefront aberration with age is a decrease in optical and visual performance, even in healthy eyes.[40]

In addition to changes in the optical aberration architecture of ocular optics, there is a significant decrease in the transmission of the eye with aging. This decrease is mainly attributable to the age-related changes of the lens, and less to the cornea. An increase in forward scatter and backscatter is a normal finding after the age of 45 years.[66,67] As cataract severity increases, however, forward scatter in the lens dominates over backscatter.

The mean decrease in pupil size under mesopic lighting conditions with aging might compensate for the overall decrease in the optical performance of the eye with aging.[68,69] A smaller pupil increases depth of field, thus improving focus and maximizing visual performance by collecting the wavefront aberration through the central area of the ocular optics. On the other hand, age-related differences in contrast sensitivity under mesopic conditions cannot be explained solely by differences in pupil diameter.[68] When a cataract is removed and spherical aberration corrected with aspheric IOLs, approximately two thirds of the population will regain the contrast sensitivity they had when they were younger.[70–72] The remaining loss in sensitivity with aging can, therefore, reflect neural changes that take place at and beyond the retinal plane.[73]

MATHEMATICAL DESCRIPTORS OF OPTICAL QUALITY IN VISION SCIENCE

If an eye could be fitted with a perfect optical system, it would focus all rays of light from a distant point source into a single image point on the retina. In this case, the only optical question is where the image point is located. To answer this question, the basic laws of paraxial (Gaussian) optical theory can be applied to describe the ideal case of perfect imaging.[74] Real eyes, on the other hand, have various optical imperfections (eg, aberrations, diffraction, scattering) that are not treated by paraxial theory. Although the mechanism is different in each case, the common effect of these imperfections is to spread light across the retina. A second, and more difficult, question is what is the spatial distribution of light intensity in the image. Answering this question requires the concepts and computational tools of Fourier analysis.[75,76] Even though the optical system of the eye is complex, the process of image formation can be simplified. The common approach to this focuses on the image-forming properties of the eye's optical system as a whole rather than on analyzing the physical and optical properties of every component of the system. The mathematics of image formation is based on the assumption that we can measure how light changes by passing through the optics of the eye.

First, before considering the single aspects of the optical and image-forming properties of the eye, it is necessary to express this information using a simple and universal language. Optical aberration measurements of the eye cannot be comparable unless they are calculated with respect to the same reference axis and expressed in the same manner. In response to a perceived need in the vision community, an Optical Society of America task force[77] was formed at the 1999 Topical Meeting on Vision Science and Its Applications meeting; the task force was charged with defining the conventions and standards for reporting optical aberrations in human eyes. From these research efforts, American National Standards Institute standard ANSI Z80.28-2004 was determined.[5] More recently, International Standards Organization standard ISO 24157:2008 was published.[6]

Two traditional axes of the eye, the visual axis and the line of sight, are centered on the foveola (Figure 2). However, only the latter passes through the pupil center. In object space, the visual axis is typically defined as the line connecting the fixation object point to the eye's first nodal point. In image space, the visual axis is the parallel line connecting the second nodal point to the center of the foveola. In contrast, the line of sight is defined as the line passing through the center of the eye's entrance pupil and exit pupil that connects the object of regard to the center of the foveola. (It does not pass through the nodal points.) The line of sight is equivalent to the path of the foveal chief ray and therefore is the axis that conforms to optical standards. The visual axis and the line of sight are not the same; in some eyes, the difference can have a significant effect on the quality of the retinal image. It is the recommendation of the Optical Society of

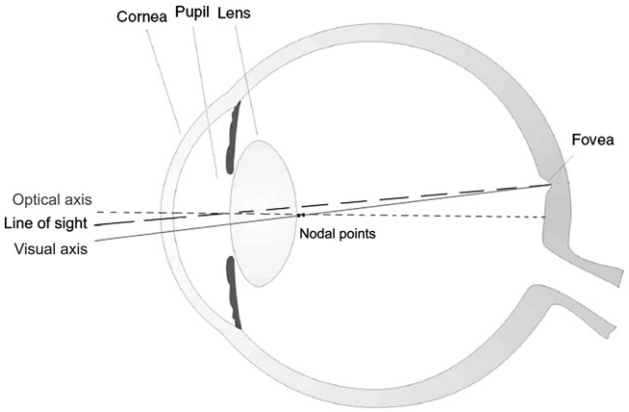

Figure 2. Schematically, the optical axis of the eye is a line joining the centers of curvature of all the optical surfaces. The appropriate and convenient axis that can be used for describing the optical system of the eye is, however, the line of sight, which is defined as the ray that passes through the center of the entrance pupil and strikes the center of the foveola. The visual axis is an axis that also strikes the foveola but passing through the nodal points of the eye. These points correspond nearly to the optical center of the refracting system, and the axis ray passing through these points is not refracted. Every ray directed to the first nodal point appears after refraction to come from the second point and continues in the same direction it first had. The nodal points in the eye are situated approximately 7.0 mm behind the cornea (just behind the lens).

America that the ophthalmic community use the line of sight as the reference axis to calculate and measure optical aberrations in the eye.[77] The rationale is that the line of sight in the normal eye is the path of the chief ray from the fixation point to the center of the retinal foveola.[78] Therefore, aberrations measured with respect to this axis will have the pupil center as the origin of a Cartesian reference frame. In this context, corneal topographers that are centered at vertex normal must translate to the center of the entrance pupil to accurately draw the corneal wavefront map.

At present, ocular aberration is usually expressed in the entrance pupil in terms of the wavefront aberration; that is, by defining how the phase of light is affected as it passes through the optical system. The wavefront is a line that joins every point on a wave that has the same phase. In other words, it is a surface that joins the leading edges of all rays at some instant. Wavefront aberration is defined as the deviation of this wavefront from a reference surface (the ideal-plane wave). The reference surface is commonly defined as a surface of curvature near the wavefront whose origin is located at the Gaussian image point (where the light would be focused if the eye were perfect). If the Gaussian image is at infinity, it follows that the reference surface is plane. For the human eye, the natural choice for the reference surface would be a sphere whose center of curvature is at photoreceptor outer segments in the retina (or Bruch membrane, where the actual reflex occurs). One can make this comparison quantitatively by measuring the distance between the reflected wavefront and the ideal wavefront, which, for convenience, we place in the (x, y) plane of the eye's entrance pupil. This distance between the actual wavefront and the pupil plane represents an optical error that varies from point to point across the pupil and therefore can be quantified by the function $W(x,y)$, which is the wave aberration function defined over the x, y coordinates of the pupil. For example, the wavefront error in an eye with defocus only has a parabolic shape that can be defined mathematically by the following equations:

$$W(x,y)=2\left(x^2+y^2\right)-1 \quad (1A)$$

or

$$W(\rho,\theta)=2\rho^2-1 \quad (1B)$$

The -1 in the equations forces the average error to be zero. It is, in general, preferable to represent wavefront errors not in terms of the x–y coordinates of a rectangular coordinate system in the pupil plane but instead in terms of polar coordinates ρ and θ. This makes the representation of other optical aberrations, such as main axis astigmatism, simpler, for example,

$$W(x,y)=y^2-x^2 \quad (2A)$$

or

$$W(\rho,\theta)=\rho^2\cos 2\theta \quad (2B)$$

as well as the representation of other asymmetric aberrations (eg, coma, trefoil).

The wavefront aberration is often defined mathematically by a series of polynomials, such as the Seidel polynomials, the Taylor polynomials or, the most popular choice for ophthalmic optics, the Zernike polynomials, which have also been recommended as the standard method for specifying wavefront error in the eye.[5,6] In general, these polynomials can be used to represent any surface, and the quality of the fit is limited only by the number of polynomial terms used.

The Zernike polynomials are a set of functions that are orthogonal in a continuous fashion over the unit circle, which means they are independent of each other mathematically. Therefore, they can be extremely useful for describing the shape of an aberrated wavefront in the pupil of a complex optical system. Several normalization and numbering schemes for these polynomials are in common use. In the following, the different schemes for presenting Zernike data as they relate to the aberration theory for the human eye are described.

The Zernike polynomials are usually defined in polar coordinates (ρ, θ), where ρ is the radial coordinate ranging from 0 to 1 and θ is the azimuthal component ranging from 0 to 2π. Each Zernike polynomial consists of 3 components: a normalization factor, a radial-dependent component, and an azimuthal-dependent component. The radial component is a polynomial, whereas the azimuthal component is sinusoidal. In general, it is recommended that a double-indexing scheme be used to describe unambiguously these functions, with the subscript index n describing the highest power (order) of the radial polynomial and the superscript index m (also described as f) describing the azimuthal (meridional or angular) frequency of the sinusoidal component (Figure 1). By convention, harmonics in cosine phase are assigned positive frequencies ($+m$) and harmonics in sine phase are assigned negative frequencies ($-m$). By this scheme, the Zernike polynomials are defined as

$$Z_n^m(\rho,\theta)=\left\{\begin{array}{l} N_n^m R_n^{|m|}(\rho)\cos m\theta;\ \text{for } m\geq 0 \\ -N_n^m R_n^{|m|}(\rho)\sin m\theta;\ \text{for } m<0 \end{array}\right\} \quad (3)$$

where N_n^m is the normalization factor, $m\theta$ (also described as M) is the azimuthal-dependent component, and $R_n^{|m|}(\rho)$, the radial-dependent component, is a polynomial function:

$$R_n^{|m|}(\rho)=\sum_{s=0}^{(n-|m|)/2}\frac{(-1)^s(n-s)!}{s![0.5(n+|m|-s)]![0.5(n-|m|-s)]!}\rho^{n-2s} \quad (4)$$

This definition uniquely describes the Zernike polynomials except for the normalization constant, that is given by

$$N_n^m=\sqrt{\frac{2(n+1)}{1+d_{m0}}} \quad (5)$$

where d_{m0} is the Kronecker delta function (ie, $\delta_{m0}=1$ for $m=0$ and $\delta_{m0}=0$ for m does not $=0$). Note that the value of n is a positive integer or zero and that for a given n, m can only take on values of $-n$, n, $+2$, $+4$,… n.

A systematic approach to classifying aberrations would be to decompose the eye's aberration architecture into Zernike polynomials that can be studied separately. The aberration structure of an eye can be then mathematically described as the weighted sum of Zernike basis functions

$$W(\rho,\theta)=\sum_{m,n}C_n^m Z_n^m(\rho,\theta) \quad (6)$$

For example

$$W(\rho,\theta)=C_2^{-2}\times Z_2^{-2}+C_2^0\times Z_2^0+C_2^{+2}\times Z_2^{+2}$$
$$+\ldots=\sum_{m,n}C_n^m Z_n^m$$

Such a description is called a Zernike expansion of the wavefront aberration. The weight C_n^m is called an aberration coefficient of the Zernike circle polynomial Z_n^m. Each individual mode (typically specified in microns or in the units of wavelength of light, λ) varies as a function of ρ and θ and is normalized and individually weighted according to its contribution to the total wavefront aberration.

A single-indexing scheme can also be used for describing Zernike expansion coefficients; for example, when designing bar plots of expansion coefficients. On the other hand, because the polynomials actually depend on 2 parameters, n and m, the ordering of a single-indexing scheme is arbitrary. To obtain the single index, j, it is convenient to lay out the polynomials in a pyramid with row number n and column number m, as shown in Table 1. The single index, j, starts at the top of the pyramid and steps down from left to right. To convert between j and the values of n and m, the following relationships can be used:

Table 1. Single-index scheme j of Zernike polynomials up to the 4th order.

	j Value of Zernike Polynomials								
	Sinusoidal Frequency m								
Polynomial Order n	−4	−3	−2	−1	0	+1	+2	+3	+4
0	—	—	—	—	0	—	—	—	—
1	—	—	—	1	—	2	—	—	—
2	—	—	3	—	4	—	5	—	—
3	—	6	—	7	—	8	—	9	—
4	10	—	11	—	12	—	13	—	14

$$\begin{aligned} j &= \tfrac{n(n+2)+m}{2}(\text{mode number}) \\ n &= roundup\left[\tfrac{-3+\sqrt{9+8j}}{2}\right](\text{radial order}) \\ m &= 2j - n(n+2)(\text{angular frequency}) \end{aligned} \quad (7)$$

An alternative scheme for describing the wavefront aberration in the eye is the magnitude/axis representation.[79] In this representation, terms are described in a fashion similar to that used to describe common spherocylindrical errors in the eye. The wavefront is represented using Zernike terms by assigning a pair of values—a magnitude and an axis—to all terms that are radially symmetric. The azimuthal terms are changed to take only 1 form instead of 2 forms and are given the form

$$A(n,m) = \cos[m\theta - \alpha_{\mathrm{nm}})] \quad (8)$$

where m can take only positive values and α_{nm} is a new variable and has a character of cylinder axis; it tells how the Zernike term is oriented with respect to the horizontal. The value of α_{nm} may be found from the coefficients associated with the standard terms $Z_{\mathrm{n}}^{\mathrm{m}}$ and $Z_{\mathrm{n}}^{\pm\mathrm{m}}$ using the equation

$$\alpha_{\mathrm{nm}} = \frac{\operatorname{atan}\left(\frac{c_{\mathrm{n}}^{-\mathrm{m}}}{c_{\mathrm{n}}^{\mathrm{m}}}\right)}{|m|} \quad (9)$$

The coefficient for the simplified scaled Zernike surface, which expresses its magnitude, is given by

$$c_{\mathrm{nm}} = \sqrt{(c_{\mathrm{n}}^{-\mathrm{m}})^2 + (c_{\mathrm{n}}^{\mathrm{m}})^2} \quad (10)$$

so that the simplified scaled Zernike surface is given by

$$S_{\mathrm{nm}}(c_{\mathrm{nm}}, \alpha_{\mathrm{nm}}) = c_{\mathrm{nm}} N_{\mathrm{n}}^{\mathrm{m}} R_{\mathrm{n}}^{\mathrm{m}} \cos[m(\theta - \alpha_{\mathrm{nm}})] \quad (11)$$

The surfaces are expressed in the form S_{nm} (c_{nm}, α_{nm}) to show that they are functions of a magnitude variable, c_{nm}, and an azimuthal variable, α_{nm}. These variables are like the familiar variables of cylinder and axis. To differentiate the simplified Zernike terms and coefficients from the standard Zernike functions and coefficients, both indices are given as subscripts (eg, Z_{00}, Z_{11}, Z_{31}), with the radial index given first. The advantage of this method of representation over the standard double-index scheme is that it can reduce the number of terms necessary to describe a wavefront up to a chosen Zernike order by a factor of almost 2. Also, terms that can be oriented, such as astigmatism, are described by 2 common values for clinicians; that is, a magnitude and an axis.

The net result of all these methods used to describe Zernike functions is, however, equivalent; that is, to represent the eye's wavefront aberration by fitting the error between the actual wavefront and the ideal wavefront with a Zernike expansion. Thanks to their properties, Zernike polynomials can lead to a fine representation of the aberration structure in the eye. The orthogonality of the Zernike basis functions makes it easy to calculate the RMS wavefront error, which is the square root of the total variance in a wavefront. Because the total variance in a wavefront is the sum of the variances of the individual Zernike modes, one can quickly identify the mode or modes having the greatest impact on the total RMS wavefront error in the eye by simply scanning the values of the coefficients. Furthermore, the wavefront error can be expressed as the sum of the RMS error when combining right eyes and left eyes into a single-population study, therefore avoiding confusion and sign discrepancies for all modes with odd symmetry about the y-axis (eg, Z_3^{-1}, Z_3^{-3}). Indeed, because bilateral symmetry in the aberration structure of eye would make $W(x,y)$ for the left eye the same as $W(-x,y)$ for the right eye,[80] a right-handed coordinate system is generally used with the coordinate origin at the center of the eye's entrance pupil. This makes the Zernike coefficients for the 2 eyes the opposite sign for all those modes, possibly leading to confusion when describing aberrations in bilateral studies.

There are, however, drawbacks of using the Zernike fitting to the wavefront aberration in the eye. Although the normalized coefficients show the relative contribution of each Zernike mode to the total wavefront error in the eye, they do not show the relative impact of each mode on visual function. In addition, when considering irregular ocular optics (eg, in eyes with keratoconus or after penetrating keratoplasty), the Zernike expansion method can be misleading and cannot accurately represent the optical properties of the eye surface,[8] resulting in an inadequate description of the image-forming properties of the eye being measured. This is because the Zernike expansion smoothes the data to find the best-fitting smooth surfaces (modes) to fit small-scale (rapid) changes in the same data. Accordingly, several metrics derived from wave aberration for the quantification of the optical quality in the eye to overcome the disadvantages of the Zernike polynomial expansion have been proposed.[10,81,82] In general, metrics of optical quality can be divided into 2 standard approaches. The first metrics describe the optical properties in the eye (pupil-plane metrics), and the second describe the effect of those properties on image quality (image-plane metrics). Image-plane metrics can be further classified based on the metrics of image quality for point objects (eg, PSF) and on the image quality for grating objects (eg, optical transfer function [OTF]). In physical optics, the PSF describes the effect of optical aberrations in the spatial domain and the OTF describes these effects in the frequency domain.[81,83]

The main difference between pupil-plane metrics and image-plane metrics is that the former describe the wavefront error in the plane of the pupil and the latter describe the wavefront error in the plane of the retina. Although the first method of representing optical aberrations can be useful as a threshold indication to determine whether the aberration will have an effect on image formation compared with a diffraction-limited case, the second approach give the clinician information about the optical image-forming properties of the eye being tested.

The most common pupil plane metric of wavefront flatness is RMS wavefront error computed over the whole pupil, RMS_w, as follows:

$$RMS_w = \left[\frac{1}{A}\int_{pupil}(W(x,y)-\overline{W})^2 dxdy\right]^{0.5} \quad (12)$$

where $W(x,y)$ is the wave aberration function defined over the x, y coordinates of the pupil, A is the pupil area, and the integration is performed over the entire pupil. Mathematically, RMS_w is the standard deviation of the values of wavefront error at various pupil locations. Excluding low levels of whole-eye aberration (<0.10 μm),[81] visual acuity decreases with an increasing RMS error value. Accordingly, RMS_w appears not to be adequate for thoroughly describing the eye's optical system, especially in highly aberrated eyes. An alternative approach for quantification of the eye's optical properties is to evaluate the fraction of the pupil area for which the aberration map is considered of good quality (ie, the critical diameter) using the critical pupil method.[10] This method examines the wavefront inside a subaperture that is concentric with the eye's pupil. A reasonable approach would quantify the wavefront aberration over a central region of the pupil because the central pupil has a larger contribution to vision as a result of the Stiles-Crawford effect.[84,85] In this way, the pupil fraction, PF_c

$$PF_c = \left[\frac{\text{critical diameter}}{\text{pupil diameter}}\right]^2 \quad (13)$$

has been shown to be a better predictor of visual quality than RMS_w.[10,81] The critical diameter is the area of the pupil for which the wavefront has a reasonably good quality. There is general agreement to consider an RMS of 0.10 μm or less as the endpoint for the critical diameter. Nevertheless, this approach does not account for the aberrations that may affect the rest of the pupil area.

The equivalent defocus is another metric alternative to the RMS_w as follows:

$$M_e = 4\pi\sqrt{3}\frac{RMS_w}{\text{pupil area}} \quad (14)$$

where M_e, the equivalent defocus, can be expressed in diopters and represents the amount of defocus required to produce the same wavefront variance produced by 1 or more HOAs. This metric was originally developed to help interpret the magnitude of HOAs,[12] and because it has been found to be largely independent of pupil diameter in normal eyes, it tends to simplify the quantification of an eye's HOA and overcomes the disadvantage of the RMS_w to change when pupil diameter changes.

The peak-to-valley (PV) difference is a pupil-plane metric closely correlated to RMS_w as follows:

$$PV = \max[W(x,y)] - \min[W(x,y)] \quad (15)$$

It represents the difference between the maximum height and minimum height of the eye's wavefront aberration. For example, if the maximum height in the positive direction were $+0.2$ μm and the maximum height in the negative direction -0.1 μm, the PV difference would be 0.3 μm. It is worth noting how the Rayleigh criterion,

$$PV < \lambda/4\theta_{min} = \frac{1.22\lambda}{d}$$

which is a traditional threshold for judging diffraction-limited optical quality, is based on PV difference, where λ is the wavelength of light, θ_{min} is the angular resolution, and d is the diameter of the entrance pupil. According to the Rayleigh criterion, in the case of green light ($\lambda = 555$ nm), the image would be significantly degraded with respect to the diffraction-limited case if the PV difference exceeds 0.14 μm (555/4). On the other hand, stating a PV difference is simply stating the maximum wavefront error; it tells nothing about the pupil area over which the error is occurring or the impact of aberrations on vision. The optical systems in 2 eyes having the same PV difference may perform differently. Therefore, the PV difference contains the same practical limitations as RMS_w. Alternatives, such as the image-plane metrics, have been therefore evaluated in recent years in an attempt to more clearly represent the optical image quality in the eye.

Optical aberrations can give rise to complex optical effects that cannot be simply quantified or mathematically characterized. In this case, one could use the point-spread information calculated using the aberration information. The optical system in a perfect eye, although diffraction limited, images a point object as a compact, high-contrast retinal image (ie, the Airy disk). An aberrated eye will form a less compact and lower contrast image on the retina because the light is blurred by the ocular optics (Figure 3). The image

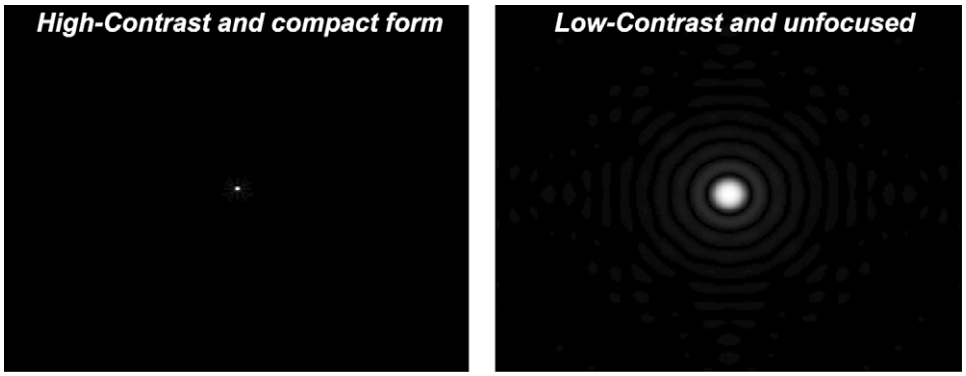

Figure 3. *A*: The retinal image of a point source in a high-quality eye has a high-contrast and compact form. *B*: In an aberrated eye, a point source produces an image with low contrast that is blurred spatially. Because the PSF is the image of a point source formed by the eye's optical system, an infinity variety of PSF images can be depicted depending on the nature and magnitude of the eye's optical aberrations.

of a point object is called a PSF, and all scalar metrics of image quality of the PSF in aberrated eyes (ie, Strehl ratio, visual Strehl ratio)[86] are designed to capture these attributes of compactness and contrast.

The PSF can be computed using the Fraunhofer approximation (ie, under far-field approximation for PSF near the image plane):

$$\mathrm{PSF}(x_i, y_i) = \mathrm{K}|\mathrm{FT}\{A(x,y)e^{-i\frac{2\pi}{\lambda}W(x,y)}\}|^2 \qquad (16)$$

where K is a constant; the squared magnitude function is the pupil function PF(x,y), which defines how light is transmitted by the eye's optics and contains information on the wave aberration $W(x,y)$ of the eye; and FT is the Fourier transform operator.

The Strehl ratio is a scalar metric that useful in describing the quality of the PSF in an eye. It is the ratio of the actual intensity (in the presence of aberrations) at the Gaussian image point to the maximum intensity of a diffraction-limited spot (if no aberrations were present) and is given by

$$\text{Strehl ratio} = \frac{1}{\pi^2}\left|\int_0^{2\pi}\int_0^1 e^{i2\pi\Delta W(\rho,\theta)}\rho d\rho d\theta\right|^2 \qquad (17)$$

where ΔW is the wave aberration relative to the reference sphere for diffraction focus. The Strehl ratio takes a number from 0 to 1; 1 defines a perfect eye's optical system. The Maréchal criterion states that a system is regarded as well corrected if the normalized intensity at diffraction focus is 0.8 or greater.[12] The drawback of the Strehl ratio is that it tends to underpredict the optical system in a low-quality eye. For low levels of aberrations (≤ 0.5), the Strehl ratio is independent of the nature of the aberration and the Strehl degradation is proportional to the variance in the wavefront aberration.

Unlike point objects, which can produce an infinity variety of PSF images depending on the nature of the eye's aberrations, grating objects always produce sinusoidal images no matter how aberrated the eye. Thus, there are only 2 ways aberrations can affect the image of a grating. They can reduce the contrast, or they can translate the image sideways to produce a spatial phase shift. Within this context, one can think of the optical system of the eye as a filter that lowers the contrast and changes the relative position of each grating in the object spectrum as it forms a degraded retinal image. The variation in image contrast with spatial frequency for an object is called MTF. The variation in image phase shift with spatial frequency is called phase transfer function (PTF). The OTF, by definition, is a complex-valued function of spatial frequency; the MTF and PTF can be derived by the OTF by taking its magnitude or taking its phase, respectively. In practice, the magnitude of the OTF is equal to the ratio of image contrast to object contrast and the phase is equal to the spatial phase difference between the image and the object (Figure 4).

The MTF plots a number from 0 to 1 (modulation) that characterizes the degradation of the image for every spatial frequency of the object sine wave. The testing object's sine wave is degraded by the eye to another sine wave characterizing the image. An MTF of 1 describes a perfect eye with no degradation. A sine wave with an MTF close to 0 completely degrades the image so that it cannot be distinguished. Therefore, the MTF tells how the contrast of the various spatial frequencies in the object is reduced in the image. In other words, the MTF describes the ability of the eye's optics to reproduce on the retina the spatial frequencies found in the visual test (eg, in a contrast sensitivity function test). In general, the MTF is a 2-dimensional function of spatial frequency and orientation, or equivalently of spatial frequency in the x-direction and the y-direction. Such function can be reduced to a 1-dimensional graph, a process called radial averaging. This process is currently used in the clinical environment to evaluate, for example, the influence of aging or a refractive procedure on visual quality.[87] To do this, the 2-dimensional mean MTF in a population study is converted from rectangular coordinates to polar coordinates and then averaged across

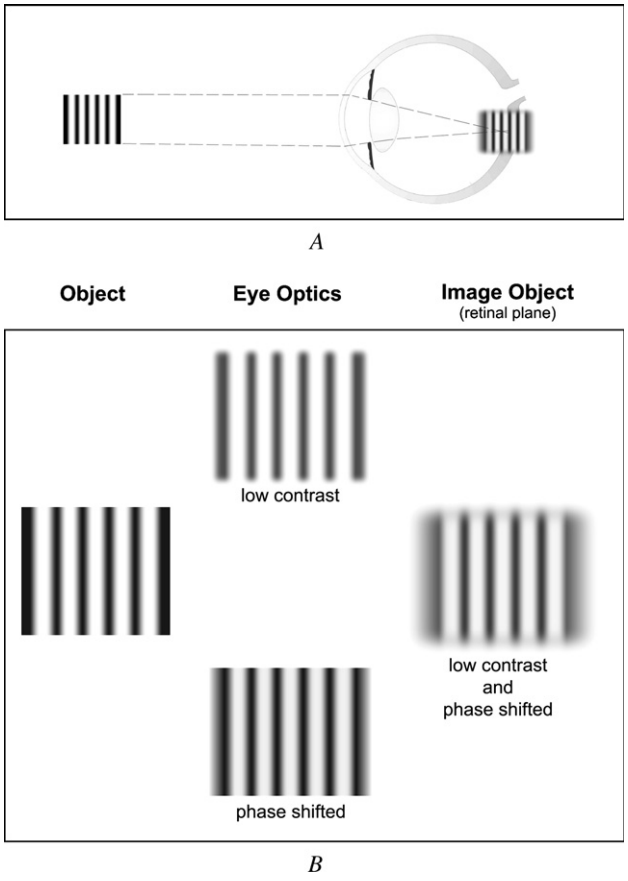

Figure 4. The use of gratings in the clinical setting allows the study of the eye's optical properties by analyzing 2 parameters: the contrast and the spatial phase. The concept of using grating objects, derived from optics and photonics performance testing, in which the brightness of the dark and light areas are changing in the form of the sine wave, is usually used in contrast sensitivity testing in the clinical environment. The particular sine wave is characterized by the spatial frequency in cycles per deg. Cycle is the width of the dark and light areas together, similar to how frequency characterizes the sine wave in mathematics. *A*: Optical aberrations in the eye degrade the retinal-image quality by reducing the contrast and inducing a shift in the spatial phase of the object. *B*: The relative effect of optical aberrations on contrast (*upper grating*, expressed by MTF) and phase shift (*lower grating*, expressed by PTF) of an object grating, with the resulting image projected onto the retina (expressed by OTF).

all meridians. Lombardo et al.[88] suggested another useful approach based on MTF metric values This approach uses a single index to describe the influence of laser refractive procedures on corneal optical quality. This parameter, namely the MTF ratio, gives an easy overall value of the effect on the eye's optical-image quality induced by surgery. A value higher than 1 means that a decline in the optical quality has occurred in ocular (or corneal, if using a corneal aberrometer) optics, whereas a value less than 1 indicates an improvement in optical quality. The MTF ratio is the ratio between the preoperative MTF and postoperative MTF for spatial frequencies up to 60 cycles per degree (cpd). In their study, Lombardo et al. found a distinct decline (nearly 14 cpd and 7 cpd with medium pupils and large pupils, respectively) in the quality of corneal optics after excimer laser surgery to correct moderate to high myopia. This result is consistent with previous theoretical work[89] and with clinical measurements of visual performance after excimer laser surgery, in which there was a decrease in contrast sensitivity function in the low and middle frequency, specifically within 6 cpd and 18 cpd, with large pupils.[90–92]

Metrics of optical quality can also include knowledge of the neural component of the visual system. The neural sharpness and the visual Strehl ratio (computed in the spatial domain) metrics are 2 examples; they weight the PSF with functions chosen to represent the neural visual system (D.R. Williams, "Subjective Image Quality Metrics From the Wave Aberration," paper presented at the 4th International Congress of Wavefront Sensing and Aberration-Free Refractive Correction, San Francisco, California, USA, February 2003).[93] The difference between neural sharpness and visual Strehl ratio is the choice of these functions. In the case of neural sharpness, the weighting function ignores light outside of the central 4 arc minutes (arc/min) of the PSF, whereas in the case of visual Strehl ratio it ignores light outside of the central 3 arc/min of the PSF to detract it from image-quality formation as follows:

$$\mathrm{NS} = \frac{\int_{\mathrm{psf}} \mathrm{PSF}(x,y)g(x,y)dxdy}{\int_{\mathrm{psf}} \mathrm{PSF}_{\mathrm{DL}}(x,y)g(x,y)dxdy} \qquad (18)$$

where NS is the neural sharpness, $g(x,y)$ is a bivariate-Gaussian neural-weighting function, and $\mathrm{PSF}_{\mathrm{DL}}$ is the diffraction-limited PSF and

$$\mathrm{VSX} = \frac{\int_{\mathrm{psf}} \mathrm{PSF}(x,y)N(x,y)dxdy}{\int_{\mathrm{psf}} \mathrm{PSF}_{\mathrm{DL}}(x,y)N(x,y)dxdy} \qquad (19)$$

where VSX is the visual Strehl ratio and $N(x,y)$ is a bivariate neural weighting function equal to the inverse Fourier transform of the neural contrast sensitivity function for interference fringes (D.R. Williams, "Subjective Image Quality Metrics from the Wave Aberration," paper presented at the 4th International Congress of Wavefront Sensing and Aberration-Free Refractive Correction, San Francisco, California, USA, February 2003). It was recently shown experimentally how the visual Strehl ratio can be a good predictor of visual acuity.[86]

After considering the objective metrics useful to describe the optical quality of the eye, we can now proceed to evaluate the effect of monochromatic

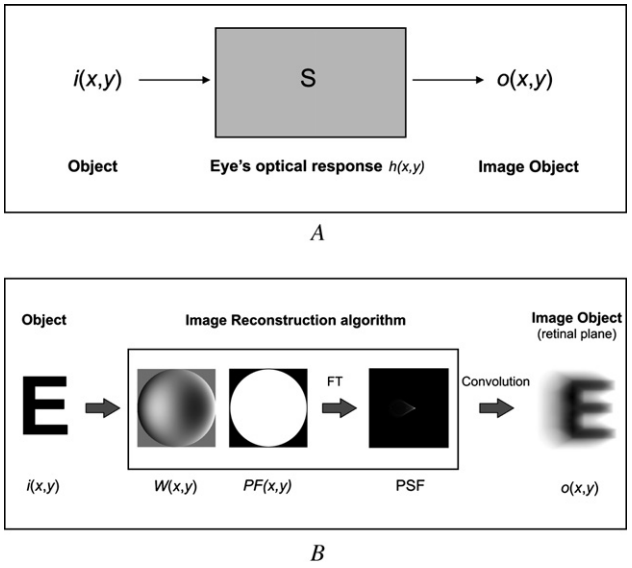

Figure 5. *A*: Detailed analysis of the optical quality in a system such as the human eye can be performed in the spatial domain and the frequency domains. Using the language of electrooptical engineering, the eye's optical system can be modeled through its response, $h(x,y)$, to a visual stimulus (ie, any object in the real world). If we suppose that the human eye optical system, S, be a linear and spatial-invariant system, any object of the external world, $i(x,y)$, will be projected by the optical system onto the retina with the corresponding image, $o(x,y)$, obtained by a mathematical operator that is a 2-dimensional convolution integral, as expressed in equation 23. In the spatial domain, the response of the eye's optical system, $h(x,y)$, to a luminous stimulus is called the PSF; in the frequency domain, this response, $H(fx,fy) = \mathrm{FT}[h(x,y)]$, is called the OTF. In other words, the PSF and the OTF are interrelated characterizations of the incoherent imaging characteristics in the eye, where $\mathrm{OTF}(fx,fy) = \mathrm{FT}[\mathrm{PSF}(x,y)]$. *B*: Image reconstruction is a powerful tool for investigating the quality of the retinal image. The preliminary step involves the objective measurement of the wavefront error function, $W(x,y)$; accordingly, when the pupil transmittance function, $PF(x,y)$, is formed, a 2-dimensional Fourier transformation is used to calculate the PSF (see equation 16). The next step is to convolve the PSF of the optical system with the object $i(x,y)$ to yield a simulation of the object at the retinal plane, $o(x,y)$. Such measurements are valid only for a fixed pupil and a fixed accommodation level. Here, the simulated image of an eye chart is represented if the eye would have only horizontal coma (Z_3^1); the $PF(x,y)$ defined a uniform light transmission inside the aperture (4.0 mm pupil).

aberrations at the retinal plane, giving details of the methods used to assess the image-forming properties in an eye and to represent the quality of the retinal image (Figure 5). These procedures can be used to simulate and predict visual performance and are performed by most current wavefront-sensor systems. It is, therefore, now possible to perform real-time image reconstruction in the consulting room. This allows clinicians to better understand a patient's visual performance. Furthermore, the image-reconstruction technique can broaden our knowledge of the effects of various forms of aberrations on retinal-image quality for complex, real-world scenes. For example, image reconstruction can be used to simulate the effects of pupil size on retinal-image quality under different light conditions or even to simulate night vision.

The preliminary step involves the objective measurement of the wavefront error function, $W(x,y)$; thus, the pupil function, $\mathrm{PF}(x,y)$, can be expressed as

$$\mathrm{PF}(x,y) = A(x,y)e^{-i\frac{2\pi}{\lambda}W(x,y)} \tag{20}$$

As mentioned, the pupil function has 2 components —an amplitude component $A(x,y)$ and a phase component that contains the wave aberration function $W(x,y)$. The $W(x,y)$ function can be expressed with Zernike polynomials; the amplitude component $A(x, y)$ defines the shape, size, and transmission of the optical system. The most common shape of the aperture function is a circ function that defines a circular aperture, which takes on a value of 1 inside the aperture and 0 outside the aperture. However, a circ function may not always be the correct choice. To model variable transmission, one can represent the pupil function as the fraction of transmitted light as a function of pupil location. For example, variable transmission can be used to model the imaging properties of the eye by incorporating phenomena such as the Stiles-Crawford effect.[84,85] In this case, the amplitude component of the pupil function takes the form of a Gaussian function. Shading of the pupil to attenuate light differentially across the pupil is called apodization.[94] It is as though the eye has a filter in the pupil plane that attenuates light near the margin of the pupil more than light passing through the center, thus reducing the impact of defocus on retinal-image quality[94] (Figure 6). The following equation can describe the Stiles-Crawford effect:

$$\eta(r) = \eta_{\max} 10^{-\rho(r - r_{\max})^2} \tag{21}$$

where η is the sensitivity to light entering the eye, r is the radial distance from the point of maximum sensitivity (considering a symmetric transmission of light through the pupil), and ρ is a space constant that affects the rate of change in sensitivity[85]: the ρ value is typically about 0.05 mm^{-2}. If the Stiles-Crawford effect is incorporated into the calculation of equation 20, the amplitude function should take the following form:

$$A(x,y) = e^{(-\rho R^2)} \tag{22}$$

Apodization in this amplitude function is achieved by using $\rho = \rho_e/2$, where ρ_e is the psychophysically determined exponent of 0.10592 mm^{-1}, which is representative of the horizontal ρ values in normal eyes.[94] R is the pupil radius and x and y are the pupil

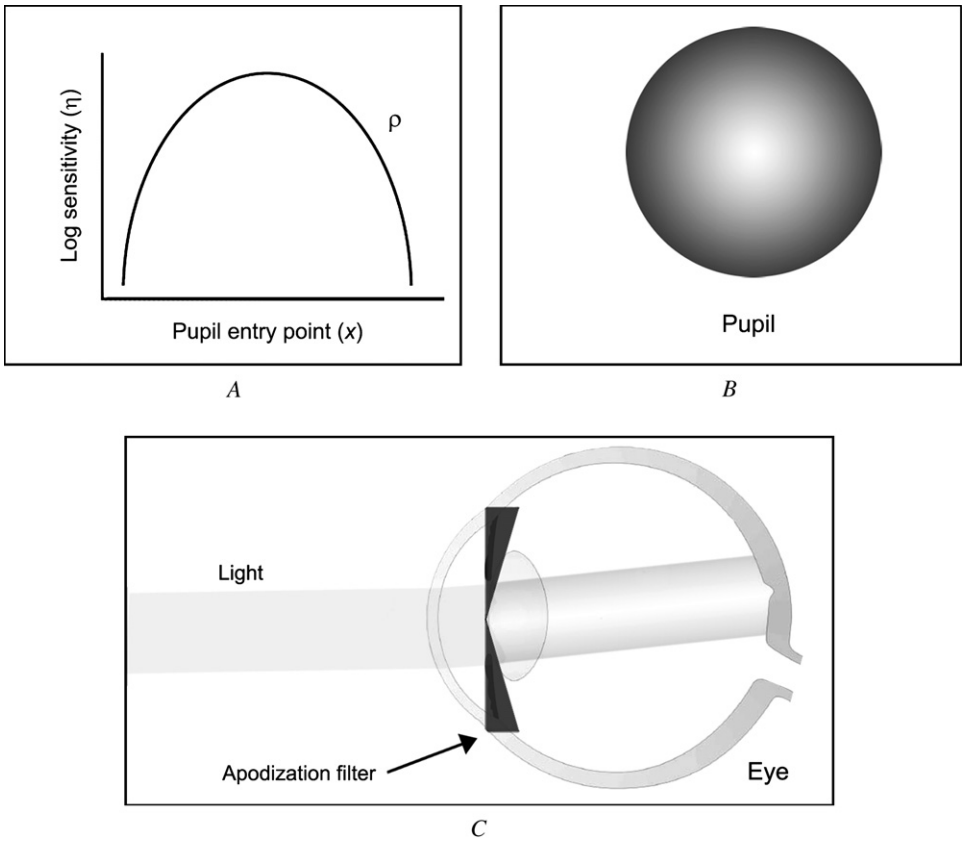

Figure 6. Schematic representation of the Stiles-Crawford effect. *A*: Visual sensitivity, η, is dependent on the radial distance between the point *x*, at which light passes through the eye's pupil, and the peak of the Stiles-Crawford effect. In equation 21, relating sensitivity to pupil location, ρ determines the steepness of this function. *B*: The transmission peak is assumed here to coincide with the pupil center. *C*: Although the origin of the Stiles-Crawford effect is retinal, it can be adequately modeled with an apodizing filter that behaves as a radially symmetric neutral density wedge in the pupil plane. The net result of the Stiles-Crawford effect is to minimize the impact of defocus on retinal image quality.

coordinates relative to the transmission peak, which is assumed to coincide with the pupil center. It has been shown, however, that the peak does not always coincide in position with the center of the pupil.[84,85] Therefore, if the Stiles-Crawford effect is used, it must be translated (shifted) to be accurate because the pupil center does not coincide with the transmission peak, which in general is nasally displaced and is mirror symmetric between right eyes and left eyes. Moreover, experimental studies[85] show that transmission at the edge of the pupil decreases exponentially with increasing pupil diameter; it ranges on average from 63% to 15% with pupil diameters between 4.0 mm to 8.0 mm. Although the apodization model described can account for the Stiles-Crawford effect, the phenomenon is known to have a retinal basis in the optical behavior of cone photoreceptors because they seem to act as optical fibers and have typical waveguide properties.[85]

Once the nature of the light transmitted by the optical system is known, the image reconstruction is relatively straightforward. In the limit where the object, $i(x,y)$, is small and composed of a single wavelength, the image at the retinal plane, $o(x,y)$, can be computed by convolving the PSF(x,y) of the optical system with the object itself as follows[75]:

$$o(x,y) = i(x,y) \otimes \mathrm{PSF}(x,y) = \iint i(\gamma,\xi) \times \mathrm{PSF}(x-\gamma, y-\xi)\, d\gamma\, d\xi \quad (23)$$

For computational reason, however, it is preferable to reconstruct the retinal image in the frequency domain, in which the convolution operator is substituted by a simple multiplication as follows:

$$O\left(f_x, f_y\right) = I\left(f_x, f_y\right) \times \mathrm{OTF}\left(f_x, f_y\right) \quad (24)$$

where $O(f_x,f_y)$is the Fourier transform of $o(x,y)$ and $I(f_x,f_y)$ is the Fourier transform of $i(x,y)$ in equation 23. Taking the inverse Fourier transform in equation 24 returns it to the space domain.

The physical basis of the equation above derives from the fact that in the frequency domain, the elemental object is not a point of light but rather a sinusoidal grating pattern. Therefore, the PSF, which expresses how the optical system spreads light about in the image plane, contains latent information on how the system attenuates the contrast and shifts the phase of component gratings. In summary, the PF, the PSF, and the OTF are interrelated characterizations of the incoherent imaging characteristics of an optical system

such as the eye. Of these, the PF is the most fundamental because it can be used to derive the other 2 metrics. The Fourier transform of the OTF is the PSF; therefore, all discussed metrics of image quality (MTF, PTF, PSF, and Strehl ratio) can be calculated from the OTF.

By including into the calculation of an image-reconstruction algorithm the weighting functions for describing the receptive fields of ganglion cells and the aliasing phenomenon, one could further model the neural transmission of the retinal image and definitely represent the image at the visual cortex plane.[83]

In addition to the monochromatic aberrations, the eye has a significant amount of chromatic aberration caused by the dispersive nature of the eye's refractive media. From a physical viewpoint, dispersion is the variation in refraction that results from the variation in the refractive index with wavelength, λ. Chromatic dispersion causes the focus, size, and position of retinal images to vary with wavelength. Metrics of optical quality do not generalize easily to the case of polychromatic light. This lack of generality is a limitation of virtual refraction based on wavefront quality. A possible approach, which would require justification, is to compute the weighted average of monochromatic metric values computed for a series of wavelength

$$\text{Metric}_{\text{poly}} = \int S(\lambda)\text{Metric}(\lambda)d\lambda \qquad (25)$$

where the weighting function $S(\lambda)$ is the luminance spectrum of the source and $\text{Metric}_{\text{poly}}$ can be one of PSF, OTF, and so forth. On the other hand, any wavelength-dependent metric should take into account the photometric human photopic or scotopic relative luminosity curves to properly weight the wavelengths. Indeed, the relative brightness of colors viewed under bright light differs from the same colors viewed under dim light; the scotopic curve peak, at 555 nm, is displaced approximately 50 μm from the photopic curve peak, at 507 nm.[95,96]

Although backward light scattering was measured in an early attempt to predict forward scatter and loss of visual performance, we are now aware that the relationship between back and forward scatter is rather complex and has to be investigated further.[97,98] However, objective measurements of forward scatter can be obtained using Hartmann-Shack or double-pass technologies[17,18,99,100] to calculate the reduction in contrast resulting from the light scattered. Several psychophysical methods have been also used to estimate disability glare caused by scattering in the eye.[97,101–103] In this context, it is acknowledged how the image contrast depends not only on the stimulus contrast but also on the stimulus luminance and geometry, background luminance, and choice of contrast definition. The choice of contrast definition is of major importance. We recommend using the Michelson definition of contrast for test gratings and the Weber definition for letter contrast tests. Indeed, the incorrect use of contrast definition can corrupt the result.[102] The Michelson contrast equation is defined by

$$M = \frac{I_{\max} - I_{\min}}{I_{\max} + I_{\min}} \qquad (26)$$

where $I_{\max}$ and $I_{\min}$ are the highest luminance and lowest luminance, respectively, and the denominator is twice the average of the luminance. The Weber contrast definition is commonly used in cases in which small features are present on a large uniform background; that is, the average luminance is approximately equal to the background luminance as follows:

$$C = \frac{I - I_b}{I_b} \qquad (27)$$

where I is the luminance of the symbol and I_b is the luminance of the immediately adjacent background. Because intraocular scatter is wavelength dependent (shorter wavelengths are scattered more than longer wavelengths),[18] for polychromatic light, a series of wavelength-dependent metrics should be defined that would account for this effect.

The theory reviewed above does not take into account the effects of diffraction and therefore is incomplete. A detailed mathematical description of diffraction is not provided here because it is beyond the scope of this work; further argument, however, can be found in the specialized literature.[75,104,105]

DISCUSSION

With the recent introduction of wavefront-related diagnostic and surgical approaches, such as adaptive optics, wavefront-guided corneal laser surgery, and personalized contact lens or IOL manufacturing, there is a need to improve the methods for measuring and representing visual performance on an individual basis in the clinical environment. Objective metrics and predictors of image and optical quality would help us better use the newly available information on the aberrations om the eye and further interpret how an induced change in aberration can influence the visual performance of an individual. Wavefront-sensing devices now represent most of the metrics and predictors of optical and retinal-image quality discussed in this review. However, the metrics discussed do not account completely for the real visual perception of an individual because vision involves many functions in addition to the optical properties of the eye, such as neural adaptation and compensation for the individual eye's optical aberrations.[106,107] Photoreceptor

sampling is another factor that may influence the correct interpretation of predictors of visual performance.

The foveal photoreceptor mosaic anatomically limits spatial resolution. Experimental studies[108,109] have found significant interindividual variability in cone packaging, ranging from 50 to 85 cpd (which corresponds to a visual acuity of 20/15 to 20/7). Therefore, one may theorize that image- and optical-quality metrics should be personalized for accurate prediction of visual performance of the eye under measurement; for example, with the use of adaptive optics. It may be unrealistic, however, to suppose that only a single metric can capture all aspects of image and optical quality; a series of metrics might be needed to adequately describe and predict the visual performance of an individual by measuring the optical properties in the eye. It remains to be determined which combination of metrics will succeed in quantifying optical quality and visual performance for a variety of visual tasks under a variety of test conditions. Although the eye can perceive spatial frequencies as high as 85 cpd, the range of spatial frequencies that is most important in everyday vision is lower, between 1 cpd and 40 cpd. A group of image-quality metrics that appreciates the importance of this range of spatial frequencies might be the best choice. Furthermore, because the natural condition of the human visual system is binocular and we live in a polychromatic world, new approaches could include examining binocular visual performance using binocular functions[110,111] and using polychromatic metrics as the best predictors of everyday visual performance.[81,112]

REFERENCES

1. Schwiegerling J. Theoretical limits to visual performance. Surv Ophthalmol 2000; 45:139–146
2. Atchison DA. Recent advances in measurement of monochromatic aberrations of human eyes. Clin Exp Optom 2005; 88:5–27
3. Lombardo M, Lombardo G. Innovative methods and techniques for sensing the wave aberrations in human eyes. Clin Exp Optom 2009; 92:176–186
4. Williams D, Yoon G-Y, Porter J, Guirao A, Hofer H, Cox I. Visual benefit of correcting higher order aberrations of the eye. J Refract Surg 2000; 16:S554–S559
5. American National Standards Institute, Inc. American National Standards for Ophthalmics – Methods for Reporting Optical Aberrations of Eyes. ANSI Z80.28, 2004;
6. International Organization for Standardization (ISO). Ophthalmic Optics and Instruments – Reporting Aberrations of the Human Eye. Geneva, Switzerland, ISO, 2008 (ISO 24157:2008)
7. Applegate RA, Ballentine C, Gross H, Sarver EJ, Sarver CA. Visual acuity as a function of Zernike mode and level of root mean square error. Optom Vis Sci 2003; 80:97–105
8. Smolek MK, Klyce SD. Zernike polynomial fitting fails to represent all visually significant corneal aberrations. Invest Ophthalmol Vis Sci 2003; 44:4676–4681. Available at: http://www.iovs.org/cgi/reprint/44/11/4676. Accessed November 11, 2009
9. Iskander DR, Collins MJ, Davis B, Carney LG. Monochromatic aberrations and characteristics of retinal image quality. Clin Exp Optom 2000; 83:315–322
10. Campbell CE. Improving visual function diagnostic metrics with the use of higher-order aberration information from the eye. J Refract Surg 2004; 20:S495–S503
11. Holladay JT, Lynn MJ, Waring GO III, Gemmill M, Keehn GC, Fielding B. The relationship of visual acuity, refractive error, and pupil size after radial keratotomy. Arch Ophthalmol 1991; 109:70–76
12. Thibos LN, Hong X, Bradley A, Cheng X. Statistical variation of aberration structure and image quality in a normal population of healthy eyes. J Opt Soc Am A Opt Image Sci Vis 2002; 19:2329–2348
13. Castejón-Mochón JF, López-Gil N, Benito A, Artal P. Ocular wave-front aberration statistics in a normal young population. Vision Res 2002; 42:1611–1617
14. Porter J, Guirao A, Cox IG, Williams DR. Monochromatic aberrations of the human eye in a large population. J Opt Soc Am A Opt Image Sci Vis 2001; 18:1793–1803
15. Charman WN, Chateau N. The prospects for super-acuity: limits to visual performance after correction of monochromatic ocular aberration. Ophthalmic Physiol Opt 2003; 23:479–493
16. Cox MJ, Atchison DA, Scott DH. Scatter and its implications for the measurement of optical image quality in human eyes. Optom Vis Sci 2003; 80:58–68
17. Artal P, Iglesisas I, López-Gil N, Green DG. Double-pass measurements of the retinal-image quality with unequal entrance and exit pupil sizes and the reversibility of the eye's optical system. J Opt Soc Am A 1995; 12:2358–2366
18. Díaz-Doutón F, Benito A, Pujol J, Arjona M, Güell JL, Artal P. Comparison of the retinal image quality with a Hartmann-Shack wavefront sensor and a double-pass instrument. Invest Ophthalmol Vis Sci 2006; 47:1710–1716. Available at: www.iovs.org/cgi/reprint/47/4/1710.pdf. Accessed November 12, 2009
19. Cerviño A, Bansal D, Hosking SL, Montés-Micó R. Objective measurement of intraocular forward light scatter using Hartmann-Shack spot patterns from clinical aberrometers; model-eye and human-eye study. J Cataract Refract Surg 2008; 34:1089–1095
20. Westheimer G, Liang J. Influence of ocular light scatter on the eye's optical performance. J Opt Soc Am A 1995; 12:1417–1424
21. Perez GM, Manzanera S, Artal P. Impact of scattering and spherical aberration in contrast sensitivity. J Vis 2009; 9(3): 19,1–10. Available at: http://www.journalofvision.org/9/3/19/Pérez-2009-jov-9-3-19.pdf. Accessed November 17, 2009
22. Levy Y, Segal O, Avni I, Zadok D. Ocular higher-order aberrations in eyes with supernormal vision. Am J Ophthalmol 2005; 139:225–228
23. Villegas EA, Alcón E, Artal P. Optical quality of the eye in subjects with normal and excellent visual acuity. Invest Ophthalmol Vis Sci 2008; 49:4688–4696
24. Cheng X, Bradley A, Hong X, Thibos LN. Relationship between refractive error and monochromatic aberrations of the eye. Optom Vis Sci 2003; 80:43–49
25. Thibos LN, Bradley A, Hong X. A statistical model of the aberration structure of normal, well-corrected eyes. Ophthalmic Physiol Opt 2002; 22:427–433
26. Salmon TO, van de Pol C. Normal-eye Zernike coefficients and root-mean-square wavefront errors. J Cataract Refract Surg 2006; 32:2064–2074

27. Wang L, Dai E, Koch DD, Nathoo A. Optical aberrations of the human anterior cornea. J Cataract Refract Surg 2003; 29:1514–1521
28. Guirao A, Porter J, Williams DR, Cox IG. Calculated impact of higher-order monochromatic aberrations on retinal image quality in a population of human eyes. J Opt Soc Am A 2002; 19:1–9; erratum, 620–628
29. Wang Y, Zhao K, Jin Y, Niu Y, Zuo T. Changes of higher order aberration with various pupil sizes in the myopic eye. J Refract Surg 2003; 19:S270–S274
30. Campbell CE. Matrix method to find a new set of Zernike coefficients from an original set when the aperture radius is changed. J Opt Soc Am A Opt Image Sci Vis 2003; 20:209–217
31. Schwiegerling J. Scaling Zernike expansion coefficients to different pupil sizes. J Opt Soc Am A Opt Image Sci Vis 2002; 19:1937–1945
32. Applegate RA, Sarver EJ, Khemsara V. Are all aberrations equal? J Refract Surg 2002; 18:S556–S562
33. Applegate RA, Marsack JD, Ramos R, Sarver EJ. Interaction between aberrations to improve or reduce visual performance. J Cataract Refract Surg 2003; 29:1487–1495
34. Artal P, Guirao A, Berrio E, Williams DR. Compensation of corneal aberrations by the internal optics in the human eye. J Vis 2001; 1(1):1–8. Available at: http://www.journalofvision.org/1/1/1/Artal-2001-jov-1-1-1.pdf. Accessed November 12, 2009
35. Artal P, Berrio E, Guirao A, Piers P. Contribution of the cornea and internal surfaces to the change of ocular aberrations with age. J Opt Soc Am A Opt Image Vis Sci 2002; 19:137–143
36. He JC, Gwiazda J, Thorn F, Held R. Wave-front aberrations in the anterior corneal surface and the whole eye. J Opt Soc Am A Opt Image Sci Vis 2003; 20:1155–1163
37. Mrochen M, Jankov M, Bueeler M, Seiler T. Correlation between corneal and total wavefront aberrations in myopic eyes. J Refract Surg 2003; 19:104–112
38. Kelly JE, Mihashi T, Howland HC. Compensation of corneal horizontal/vertical astigmatism, lateral coma, and spherical aberration by internal optics of the eye. J Vision 2004; 4(4):262–271. Available at: http://journalofvision.org/4/4/2. Accessed November 12, 2009
39. Marcos S. Are changes in ocular aberrations with age a significant problem for refractive surgery? J Refract Surg 2002; 18:S572–S578
40. Guirao A, González C, Redondo M, Geraghty E, Norrby S, Artal P. Average optical performance of the human eye as a function of age in a normal population. Invest Ophthalmol Vis Sci 1999; 40:203–213. Available at: http://www.iovs.org/cgi/reprint/40/1/203.pdf. Accessed November 12, 2009
41. Guirao A, Redondo M, Artal P. Optical aberrations of the human cornea as a function of age. J Opt Soc Am A Opt Image Sci Vis 2000; 17:1697–1702
42. Medina A, Fariza E. Emmetropization as a first-order feedback system. Vision Res 1993; 33:21–26
43. Artal P, Benito A, Tabernero J. The human eye is an example of robust optical design. J Vis 2006; 6:1–7. Available at: http://journalofvision.org/6/1/1/Artal-2006-jov-6-1-1.pdf. Accessed November 12, 2009
44. Brunette I, Bueno JM, Parent M, Hamam H, Simonet P. Monochromatic aberrations as a function of age, from childhood to advanced age. Invest Ophthalmol Vis Sci 2003; 44:5438–5446. Available at: http://www.iovs.org/cgi/reprint/44/12/5438.pdf. Accessed November 12, 2009
45. Wang J, Candy TR. Higher order monochromatic aberrations of the human infant eye. J Vis 2005; 5:543–555. Available at: http://www.journalofvision.org/5/6/6/Wang-2005-jov-5-6-6.pdf. Accessed November 12, 2009
46. McKendrick AM, Brennan NA. The axis of astigmatism in right and left eye pairs. Optom Vis Sci 1997; 74:668–675
47. Bogan SJ, Waring GO III, Ibrahim O, Drews C, Curtis L. Classification of normal corneal topography based on computer-assisted videokeratography. Arch Ophthalmol 1990; 108:945–949
48. Myrowitz EH, Kouzis AC, O'Brien TP. High interocular corneal symmetry in average simulated keratometry, central corneal thickness, and posterior elevation. Optom Vis Sci 2005; 82:428–431
49. Liu Z, Huang AJ, Pflugfelder SC. Evaluation of corneal thickness and topography in normal eyes using the Orbscan corneal topography system. Br J Ophthalmol 1999; 83:774–778. Available at: http://www.ncbi.nlm.nih.gov/pmc/articles/PMC1723104/pdf/v083p00774.pdf. Accessed November 12, 2009
50. Wang L, Koch DD. Ocular higher-order aberrations in individuals screened for refractive surgery. J Cataract Refract Surg 2003; 29:1896–1903
51. Lombardo M, Lombardo G, Serrao S. Interocular high-order corneal wavefront aberration symmetry. J Opt Soc Am A Opt Image Sci Vis 2006; 23:777–787
52. Wang L, Santaella RM, Booth M, Koch DD. Higher-order aberrations from the internal optics of the eye. J Cataract Refract Surg 2005; 31:1512–1519
53. Marcos S, Burns SA. On the symmetry between eyes of wavefront aberration and cone directionality. Vision Res 2000; 40:2437–2447
54. Jiménez Cuesta JR, Anera RG, Jiménez R, Salas C. Impact of interocular differences in corneal asphericity on binocular summation. Am J Ophthalmol 2003; 135:279–284
55. Hofer H, Artal P, Singer B, Aragon JL, Williams DR. Dynamics of the eye's wave aberration. J Opt Soc Am A Opt Image Sci Vis 2001; 18:497–506
56. Cheng H, Barnett JK, Vilupuru AS, Marsack JD, Kasthurirangan S, Applegate RA, Roorda A. A population study on changes in wave aberrations with accommodation. J Vision 2004; 4:272–280. Available at: http://www.journalofvision.org/4/4/3/Cheng-2004-jov-4-4-3.pdf. Accessed November 12, 2009
57. Iida Y, Shimizu K, Ito M, Suzuki M. Influence of age on ocular wavefront aberration changes with accommodation. J Refract Surg 2008; 24:696–701
58. Plainis S, Ginis HS, Pallikaris A. The effect of ocular aberrations on steady-state errors of accommodative response. J Vision 2005; 5:466–477. Available at: http://www.journalofvision.org/5/5/7/Plainis-2005-jov-5-5-7.pdf. Accessed November 12, 2009
59. Thibos LN. The prospects for perfect vision. J Refract Surg 2000; 16:S540–S546
60. Calver RI, Cox MJ, Elliot DB. Effect of aging on the monochromatic aberrations of the human eye. J Opt Soc Am A Opt Image Sci Vis 1999; 16:2069–2078
61. Fujikado T, Kuroda T, Ninomiya S, Maeda N, Tano Y, Oshika T, Hirohara Y, Mihashi T. Age-related changes in ocular and corneal aberrations. Am J Ophthalmol 2004; 138:143–146
62. Amano S, Amano Y, Yamagami S, Miyai T, Miyata K, Samejima T, Oshika T. Age-related changes in corneal and ocular higher-order wavefront aberrations. Am J Ophthalmol 2004; 137:988–992
63. Kuroda T, Fujikado T, Ninomiya S, Maeda N, Hirohara Y, Mihashi T. Effect of aging on ocular light scatter and higher order aberrations. J Refract Surg 2002; 18:S598–S602
64. Oshika T, Klyce SD, Applegate RA, Howland HC. Changes in corneal wavefront aberrations with aging. Invest Ophthalmol

Vis Sci 1999; 40:1351–1355. Available at: http://www.iovs.org/cgi/reprint/40/7/1351.pdf. Accessed November 12, 2009
65. Shahidi M, Yang Y. Measurements of ocular aberrations and light scatter in healthy subjects. Optom Vis Sci 2004; 81:853–857
66. Fujisawa K, Sasaki K. Changes in light scattering intensity of the transparent lenses of subjects selected from population-based surveys depending on age: analysis through Scheimpflug images. Ophthalmic Res 1995; 27:89–101
67. Hemenger RP. Intraocular light scatter in normal visual loss with age. Appl Opt 1984; 23:1972–1974
68. Sloane ME, Owsley C, Alvarez SL. Aging, senile miosis and spatial contrast sensitivity at low luminance. Vision Res 1988; 28:1235–1246
69. Winn B, Whitaker D, Elliott DB, Phillips NJ. Factors affecting light-adapted pupil size in normal human subjects. Invest Ophthalmol Vis Sci 1994; 35:1132–1137. Available at: http://www.iovs.org/cgi/reprint/35/3/1132.pdf. Accessed November 12, 2009
70. Holladay JT, Piers PA, Koranyi G, van der Mooren M, Norrby NES. A new intraocular lens design to reduce spherical aberration of pseudophakic eyes. J Refract Surg 2002; 18:683–691
71. Packer M, Fine IH, Hoffman RS, Piers PA. Improved functional vision with a modified prolate intraocular lens. J Cataract Refract Surg 2004; 30:986–992
72. Mester U, Dillinger P, Anterist N. Impact of a modified optic design on visual function: clinical comparative study. J Cataract Refract Surg 2003; 29:652–660
73. Elliott SL, Choi SS, Doble N, Hardy JL, Evans JW, Werner JS. Role of high-order aberrations in senescent changes in spatial vision. J Vis 2009; 9(2): 24,1–16. Available at: http://www.journalofvision.org/9/2/24/Elliott-2009-jov-9-2-24.pdf. Accessed November 12, 2009
74. Smith WJ. Modern Optical Engineering; the Design of Optical Systems 3rd ed. New York, NY, McGraw-Hill, 2000; 21–59
75. Goodman JW. Introduction to Fourier Optics 2nd ed. New York, NY, McGraw-Hill, 1996; 32–95
76. Iizuka K. Elements of Photonics. Volume 1. In: Free Space and Special Media. New York, NY, Wiley, 2002; 1–108
77. Thibos LN, Applegate RA, Schwiegerling JT, Webb R. Standards for reporting the optical aberrations of eyes; VSIA Standards Taskforce Members. J Refract Surg 2002; 18:S652–S660
78. Applegate RA, Thibos LN, Twa MD, Sarver EJ. Importance of fixation, pupil center, and reference axis in ocular wavefront sensing, videokeratography, and retinal image quality. J Cataract Refract Surg 2009; 35:139–152
79. Campbell CE. A new method for describing the aberrations of the eye using Zernike polynomials. Optom Vis Sci 2003; 80:79–83
80. Smolek MK, Klyce SD, Sarver EJ. Inattention to nonsuperimposable midline symmetry causes wavefront analysis error. Arch Ophthalmol 2002; 120:439–447
81. Marsack JD, Thibos LN, Applegate RA. Metrics of optical quality derived from wave aberrations predict visual performance. J Vision 2004; 4:322–328. Available at: http://www.journalofvision.org/4/4/8/Marsack-2004-jov-4-4-8.pdf. Accessed November 12, 2009
82. Thibos LN, Hong X, Bradley A, Applegate RA. Accuracy and precision of objective refraction from wavefront aberrations. J Vis 2004; 4(4):329–351. Available at: http://www.journalofvision.org/4/4/9/Thibos-2004-jov-4-4-9.pdf. Accessed November 12, 2009
83. Cheng X, Thibos LN, Bradley A. Estimating visual quality from wavefront aberration measurements. J Refract Surg 2003; 19:S579–S584
84. Stiles WS, Crawford BH. The luminous efficiency of rays entering the eye pupil at different points. Proc R Soc Lond [Biol] 1933; 112:428–450
85. Applegate RA, Lakshminarayanan V. Parametric representation of Stiles-Crawford functions: normal variation and peak location and directionality. J Opt Soc Am A 1993; 10:1611–1623
86. Cheng X, Bradley A, Thibos LN. Predicting subjective judgment of best focus with objective image quality metrics. J Vis 2004; 4:310–321. Available at: http://www.journalofvision.org/4/4/7/Cheng-2004-jov-4-4-7.pdf. Accessed November 12, 2009
87. Guirao A, Redondo M, Geraghty E, Piers P, Norrby S, Artal P. Corneal optical aberrations and retinal image quality in patients in whom monofocal intraocular lenses were implanted. Arch Ophthalmol 2002; 120:1143–1151
88. Lombardo M, Lombardo G, Serrao S. Long-term optical quality of the photoablated cornea. J Opt Soc Am A Opt Image Sci Vis 2007; 24:588–596
89. Jiménez JR, Anera RG, Jiménez del Barco L. Effects on visual function of approximations of the corneal-ablation profile during refractive surgery. Appl Opt 2001; 40:2200–2205
90. Montés-Micó R, Charman WN. Choice of spatial frequency for contrast sensitivity evaluation after corneal refractive surgery. J Refract Surg 2001; 17:646–651
91. Quesnel N-M, Lovasik JV, Ferremi C, Boileau M, Ieraci C. Laser in situ keratomileusis for myopia and the contrast sensitivity function. J Cataract Refract Surg 2004; 30:1209–1218
92. Artal P, Ferro M, Miranda I, Navarro R. Effects of aging in retinal image quality. J Opt Soc Am A 1993; 10:1656–1662
93. Campbell FW, Green DG. Optical and retinal factors affecting visual resolution. J Physiol 1965; 181:576–593. Available at: http://www.ncbi.nlm.nih.gov/pmc/articles/PMC1357668/pdf/jphysiol01162-0132.pdf. Accessed November 17, 2009
94. Zhang X, Ye M, Bradley A, Thibos L. Apodization by the Stiles-Crawford effect moderates the visual impact of retinal image defocus. J Opt Soc Am A Opt Image Vis Sci 1999; 16:812–820
95. Wyszecki G, Stiles WS. Color Science; Concepts and Methods, Quantitative Data and Formulae, 2nd ed. New York, NY, John Wiley & Sons, 1982
96. Smith T, Guild J. The C.I.E. colorimetric standards and their use. Trans Opt Soc 1931; 33:73–134
97. De Waard PWT, IJspeert JK, van den Berg TJTP, de Jong PTVM. Intraocular light scattering in age-related cataracts. Invest Ophthalmol Vis Sci 1992; 33:618–625. Available at: http://www.iovs.org/cgi/reprint/33/3/618.pdf. Accessed November 12, 2009
98. Fujikado T, Kuroda T, Maeda N, Ninomiya S, Goto H, Tano Y, Oshika T, Hirohara Y, Mihashi T. Light scattering and optical aberrations as objective parameters to predict visual deterioration in eyes with cataract. J Cataract Refract Surg 2004; 30:1198–1208
99. Donnelly WJ III, Pesudovs K, Marsack JD, Sarver EJ, Applegate RA. Quantifying scatter in Shack-Hartmann images to evaluate nuclear cataract. J Refract Surg 2004; 20:S515–S522
100. Donnelly WJ III, Applegate RA. Influence of exposure time and pupil size on a Shack-Hartmann metric of forward scatter. J Refract Surg 2005; 21:S547–S551. Available at: http://www.ncbi.nlm.nih.gov/pmc/articles/PMC1764495/pdf/nihms-12939.pdf. Accessed November 12, 2009
101. Elliott DB, Bullimore MA. Assessing the reliability, discriminative ability, and validity of disability glare tests. Invest Ophthalmol Vis Sci 1993; 34:108–119. Available at: http://www.iovs.org/cgi/reprint/34/1/108.pdf. Accessed November 12, 2009

102. Thaung J, Beckman C, Abrahamsson M, Sjöstrand J. The 'light scattering factor.' Importance of stimulus geometry, contrast definition, and adaptation. Invest Ophthalmol Vis Sci 1995; 36:2313–2317. Available at: http://www.iovs.org/cgi/reprint/36/11/2313. Accessed November 12, 2009
103. Paulsson L-E, Sjöstrand J. Contrast sensitivity in the presence of a glare light; theoretical concepts and preliminary clinical studies. Invest Ophthalmol Vis Sci 1980; 19:401–406. Available at: http://www.iovs.org/cgi/reprint/19/4/401. Accessed November 12, 2009
104. Born M, Wolf E. Principles of Optics; Electromagnetic Theory of Propagation, Interference and Diffraction of Light, 7th expanded ed. Cambridge, UK, Cambridge University Press, 1999; 412–516
105. Römer H. Theoretical Optics; An Introduction. Weinheim, Germany, Wiley-VCH Verlag, 2005; 171–206. Available at: http://books.google.com/books?id=tSFspYkrR-8C&pg=PR3&lpg=PR3&dq=%22Theoretical+Optics%3B +An+Introduction%22&source=bl&ots=SmhNJBnvNV&sig=kMKX8tlcqpFjlOzGpSHirGPDyYo&hl=en&ei=lBD8St3CHIGKnQfSjI2aBQ&sa=X&oi=book_result&ct=result&resnum=1&ved=0CAgQ6AEwAA#v=onepage&q=&f=false. Accessed November 12, 2009
106. Artal P, Chen L, Fernández EJ, Singer B, Manzanera S, Williams DR. Neural compensation for the eye's optical aberrations. J Vision 2004; 4:281–287. Available at: http://journalofvision.org/4/4/4/Artal-2004-jov-4-4-4.pdf. Accessed November 12, 2009
107. Artal P, Chen L, Fernandez EJ, Singer B, Manzanera S, Williams DR. Adaptive optics for vision: the eye's adaptation to point spread function. J Refract Surg 2003; 19:S585–S587
108. Williams DR, Coletta NJ. Cone spacing and the visual resolution limit. J Opt Soc Am A 1987; 4:1514–1523
109. Hughes A. Seeing cones in living eyes. Nature 1996; 380:393–394
110. Jiménez JR, Castro JJ, Hita E, Anera RG. Upper disparity limit after LASIK. J Opt Soc Am A Opt Image Sci Vis 2008; 25:1227–1231
111. Jiménez JR, Castro JJ. R Jiménez, Hita E. Interocular differences in higher-order aberrations on binocular visual performance. Optom Vis Sci 2008; 85:174–179
112. Ravikumar S, Thibos LN, Bradley A. Calculation of retinal image quality for polychromatic light. J Opt Soc Am A Opt Image Sci Vis 2008; 25:2395–2407

First author:
Marco Lombardo, MD, PhD
Vision Engineering, Rome, Italy